J. Radiat. Res., 51, 707–713 (2010)

Regular Paper

Depth Scaling of Solid Phantom for Intensity Modulated Radiotherapy Beams

Yukio FUJITA[1]*, Naoki TOHYAMA[2], Atsushi MYOJOYAMA[1] and Hidetoshi SAITOH[1]

Solid phantom/Depth scaling/Beam hardening effect/Multileaf collimator/Intensity modulated radiotherapy.

To reduce the uncertainty of absorbed dose for high energy photon beams, water has been chosen as a reference material by the dosimetry protocols. However, solid phantoms are used as media for absolute dose verification of intensity modulated radiotherapy (IMRT). For the absorbed dose measurement, the fluence scaling factor is used for converting an ionization chamber reading in a solid phantom to absorbed dose to water. Furthermore the depth scaling factor is indispensable in determining the fluence scaling factor. For IMRT beams, a photon energy spectrum is varied by transmitting through a multileaf collimator and attenuating in media. However, the effects of spectral variations on depth scaling have not been clarified yet. In this study, variations of photon energy spectra were determined using the EGS Monte Carlo simulation. The depth scaling factors for commercially available solid phantoms were determined from effective mass attenuation coefficients using photon energy spectra. The results clarified the effect of spectral variation on the depth scaling and produced an accurate scaling method for IMRT beams.

INTRODUCTION

For the recent national and international dosimetry protocols, water has been chosen as a reference material. However, dose measurement in water is sometimes impractical, so a solid phantom is used as a substitute for water. An example is dosimetric quality assurance of intensity modulated radiotherapy (IMRT) because a solid phantom is easier to set up than water and it can reproduce complex geometry such as anthropomorphic phantoms.

For photon beams, Seuntjens *et al.* reported a method to determine absorbed dose to water by ionization chamber measurement in solid phantoms.[1)] In their report, the "phantom dose conversion factor" is used to convert an ionization chamber reading in a solid phantom to absorbed dose to water. The factor is also known as the fluence scaling factor in the IAEA TRS-398.[2)] The factor can be determined experimentally as a ratio of ionization chamber reading in water at a reference depth to reading in a solid phantom at an equivalent depth. The equivalent depth was determined by applying the scaling theorem.[2,3)] In their report, depth can be scaled using a constant ratio of electron densities of two media. The scaling theorem assumes that photons interact with a medium only by the Compton scatter even if the pair-production accounts for 20% of total interaction for 10 MeV photon in water. Therefore, all phenomena of interactions with a medium should be considered for the depth scaling for megavoltage photon beams.

For IMRT beams, photon energy spectra are varied by transmitting through a multileaf collimator (MLC) and scattered photons in a medium. However, these effects on the depth scaling and the fluence scaling have not been clarified yet. In particular the depth scaling factor is indispensable in determining the fluence scaling factor.

The purpose of this study is to clarify effect of spectral variation on the depth scaling and to provide an accurate scaling method for IMRT beams. For this purpose, variations of photon energy spectra were obtained using the EGS Monte Carlo simulation. The depth scaling factors for commercially available solid phantoms were determined from effective mass attenuation coefficients using the photon energy spectra. The results clarified effect of spectral variation on the depth scaling.

*Corresponding author: Phone: +81(3)3819-1211,
Fax: +81(3)3819-1406,
E-mail: fujita-yukio@hs.tmu.ac.jp
[1]Graduate School of Human Health Sciences, Tokyo Metropolitan University, Higashiogu 7-2-10, Arakawaku, Tokyo 116-8551, Japan; [2]Chiba Cancer Center, Nitonachou 666-2, Chuouku, Chiba 260-8717, Japan.
doi:10.1269/jrr.10058

METHODS AND MATERIAL

Solid phantoms

In this study, as commercially available solid phantoms, WT1 (GAMMEX RMI, Wisconsin, USA), 457-CTG (GAMMEX RMI, Wisconsin, USA), RW3 (PTW, Freiburg, Germany), MixDP,[4] WE211 (Kyoto Kagaku, Kyoto, Japan), WE211R (Kyoto Kagaku, Kyoto, Japan), Plastic Water (CIRS, Virginia, USA), Plastic Water DT (CIRS, Virginia, USA), Virtual Water (Med-Cal, Wisconsin, USA), polystyrene, polymethyl methacrylate (PMMA) and acrylonitrile butadiene styrene (ABS) were evaluated. The elemental compositions, physical densities, electron densities and effective atomic numbers are summarized in Table 1.[2,5–7] The electron density ρ_e [g^{-1}] was calculated by,

$$\rho_e = \sum_i \frac{N_A w_i Z_i}{A_i} \quad (1)$$

where N_A is the Avogadro constant, w_i is fraction by weight, Z_i is atomic number and A_i is molar mass of i-th element, respectively. The effective atomic number Z_{eff} for the pair production was calculated as follows.[8]

$$Z_{eff} = \sum_i w_i Z_i \quad (2)$$

Depth scaling for photon beam

When monoenergetic photons with an incident fluence Φ_0 penetrate a layer with a mass attenuation coefficient μ/ρ and area density z, fluence behind the layer Φ is given by the following exponential attenuation law.

$$\frac{\Phi}{\Phi_0} = \exp[-(\mu/\rho)z] \quad (3)$$

If the ratio of photon fluence was equal at z_w in water and z_{pl} in a solid phantom, next relation will be established.

$$z_w = z_{pl}\frac{(\mu/\rho)_{pl}}{(\mu/\rho)_w} = z_{pl}(\mu/\rho)_{pl,w} \quad (4)$$

The term of $(\mu/\rho)_{pl,w}$ is redefined as the depth scaling factor c_{pl}. Thus, z_w can be determined by following equation.

$$z_w = c_{pl} z_{pl} \quad (5)$$

Calculation of depth scaling factor c_{pl} for megavoltage photon beam

Megavoltage photon beam produced by linear accelerator (linac) has a continuous energy spectrum, consequently, an effective mass attenuation coefficient is suitable for the depth scaling. The effective mass attenuation coefficient $\overline{\mu/\rho}$ can be obtained from a depth dose distribution such as

Table 1. The elemental compositions, physical densities, electron densities and relative electron densities for solid phantoms.[2,5–7]

Elements	Water	WT1	457-CTG	RW3	MixDP	WE211	WE211R	Plastic Water	Plastic Water DT	Virtual Water	Polystyrene	PMMA	ABS [a]
H	0.1119	0.0810	0.0810	0.0759	0.1277	0.0821	0.0838	0.0779	0.0740	0.0770	0.0774	0.0805	0.0810
B									0.0226				
C		0.6720	0.6720	0.9041	0.7682	0.6633	0.6738	0.5982	0.4670	0.6874	0.9226	0.5998	0.8490
N		0.0240	0.0240			0.0221	0.0219	0.0178	0.0156	0.0227			0.0700
O	0.8881	0.1990	0.1990	0.0080	0.0511	0.2065	0.1953	0.2357	0.3352	0.1886		0.3196	
Mg					0.0386				0.0688				
Al									0.0140				
Cl		0.0010	0.0010			0.0040	0.0024	0.0023	0.0024	0.0013			
Ca		0.0230	0.0230			0.0220	0.0228	0.0676		0.0231			
Ti				0.0120	0.0144								
ρ [g cm^{-3}]	0.998 [b]	1.020	1.043	1.045	1.000	1.018	1.018	1.030	1.039	1.030	1.060	1.190	1.050
ρ_e [$\times 10^{23}$ g^{-1}]	3.343	3.249	3.249	3.231	3.382	3.252	3.257	3.238	3.218	3.237	3.238	3.248	3.249
$(\rho_e)_{pl,w}$		0.972	0.972	0.966	1.012	0.973	0.974	0.969	0.963	0.968	0.969	0.972	0.972
Z_{eff} [c]	7.22	6.35	6.35	5.83	6.38	6.34	7.07	6.83	6.83	6.35	5.61	6.24	5.67

[a] Private letter given by Taisei Medical.
[b] The density for pure water at 22.0°C.
[c] The effective atomic number for pair production.

tissue-phantom ratio (TPR). The *TPR* for field size *A* and depth *z* can be expressed by following equation approximately.

$$TPR(z,A)=\exp\left[-(\bar{\mu}/\rho)(z-z_{ref})\right] \quad (6)$$

where z_{ref} is reference depth of TPR data. The reference depth is used for normalization of the TPR data. Thus, $\bar{\mu}/\rho$ can be determined by exponential approximation of TPR data.

However, to investigate influence of spectral variation for the depth scaling factor in detail, the $\bar{\mu}/\rho$ for several phantom materials were determined from photon energy spectra in this study. The $\bar{\mu}/\rho$ was calculated by,

$$\bar{\mu}/\rho=\frac{\int_{E_{min}}^{E_{max}}\Psi(E)[\mu(E)/\rho]dE}{\int_{E_{min}}^{E_{max}}\Psi(E)dE} \quad (7)$$

where $\Psi(E)$ is the differential energy fluence and $\mu(E)/\rho$ is the mass attenuation coefficient at photon energy E.[9] The photon energy spectra were determined by Monte Carlo methods as described in the next sub-section. The depth scaling factors were determined by following equation.

$$c_{pl}=\frac{(\bar{\mu}/\rho)_{pl}}{(\bar{\mu}/\rho)_{w}} \quad (8)$$

Monte Carlo simulation

Simulation of medical linear accelerator

The BEAMnrc code[10] was used to simulate a photon beam of Varian Clinac equipped with the Millennium 120 MLC (Varian Medical Systems, Palo Alto, CA). The geometrical data and material specifications were provided by the manufacturer. The accelerator head consists of several structures such as a target, primary collimator, vacuum window, flattening filter, secondly collimator and MLC. The MLC is composed of 80 inner leaves and 40 outer leaves whose projected width is 0.5 cm or 1.0 cm at the isocenter, respectively. The MLC was modeled by using the DYNVMLC component module.[10,11] The leaves are made of a tungsten alloy whose physical density ranges from 17.0 to 18.5 g cm^{-3} depending on the alloy composition and leaf manufacturing.[12] The density was adjusted by comparison between measured and calculated MLC transmission factor and 17.7 g cm^{-3} was employed in this report.

In this study, nominal photon energies of 4, 6, 10 and 15 MV were simulated. The initial electron energy and special distributions on the target were adjusted by comparing calculated and measured central axis depth dose and off-axis ratio in water.[13,14]

Calculation of photon energy spectra in phantom

The FLURZnrc code[15] was used to calculate photon spectra in a phantom. A phantom of height 30.0 cm and radius 20.0 cm was used for all simulation conditions. For sampling photon energy, cylindrical volume with height 0.2 cm and radius 0.2 cm were employed. The distance from source to the sampling region was fixed at 100 cm. The simulations were repeated until to get a statistical uncertainty of less than 1.0%. To clarify photon energy dependency of the depth scaling factor, photon energy spectra in each phantom for several photon energies, several depths and various field sizes were simulated.

For IMRT beams, the non-uniform fluence distribution is delivered by combining multi-segmental MLC field or sweeping MLC field. The variation of photon energy spectrum depends on the contribution of photons transmitted through the MLC. Namely completely blocked field by the MLC (blocked field) may show maximum variation of energy spectrum and maximum difference of the depth scaling factor is also expected. Therefore, the photon energy spectrum for the blocked field was also simulated.

RESULTS AND DISCUSSIONS

Photon energy dependence

The depth scaling factors for several photon energies and the relative electron densities are tabulated in Table 2. The depth scaling factors were determined from photon energy spectra at 10 cm depth with a 10 cm × 10 cm open field. For 4 MV and 6 MV, the depth scaling factors were almost equal to the relative electron density. However, for 10 MV and 15 MV, the depth scaling factors were varied from the relative electron density, except the Plastic Water. This is because the contribution of the pair-production is increased as photon energy increase. Figure 1 shows Compton and pair-production mass attenuation coefficients for the solid phantoms. These data were calculated by NIST's XCOM program.[16] The Compton mass attenuation coefficient is proportional to electron density and electron densities of solid phantoms are designed to be almost equal to water as shown in Table 1. Therefore, the Compton mass attenuation coefficients of the solid phantoms are equal to water as shown in Fig. 1-(a). In contrast, as shown in Fig. 1-(b), the pair-production mass attenuation coefficient of the solid phantom is different from water because of difference of the Z_{eff}. In particular, the depth scaling factors for the RW3, MixDP, polystyrene, PMMA and ABS showed significant variations from the relative electron density. Above all, the polystyrene showed lager difference between the depth scaling factor and relative electron density than the others. When the z_{pl} is calculated from equitation (5), the difference becomes 2.0 mm at 10 cm depth. By contrast, the Plastic Water had a constant depth scaling factor even though photon energy increases because it has the same pair-production and Compton mass attenuation coefficient as water.

Therefore, for solid phantoms which have a large difference in the Z_{eff}, the depth scaling factor should be deter-

Table 2. Depth scaling factors for the open and blocked field and relative electron densities of commercially available solid phantoms. The depth scaling factors are determined from photon energy spectra at 10 cm depth for 10 cm × 10 cm open and blocked field, respectively.

Phantom	$(\rho_e)_{pl,w}$	Nominal photon energy [MV]							
		4		6		10		15	
		Open	*MBF	Open	MBF	Open	MBF	Open	MBF
WT1	0.972	0.971	0.970	0.970	0.969	0.967	0.966	0.964	0.965
457-CTG	0.972	0.971	0.970	0.970	0.969	0.967	0.966	0.964	0.965
RW3	0.966	0.965	0.964	0.964	0.962	0.958	0.957	0.953	0.954
MixDP	1.012	1.010	1.009	1.008	1.006	1.001	1.000	0.996	0.997
WE211	0.973	0.972	0.972	0.971	0.970	0.968	0.967	0.965	0.966
WE211R	0.974	0.974	0.973	0.973	0.972	0.969	0.969	0.966	0.967
Plastic Water	0.969	0.970	0.970	0.970	0.970	0.970	0.970	0.970	0.970
Plastic Water DT	0.963	0.963	0.963	0.962	0.962	0.962	0.962	0.961	0.961
Virtual Water	0.968	0.968	0.967	0.967	0.966	0.963	0.963	0.961	0.961
Polystyrene	0.969	0.967	0.966	0.965	0.963	0.958	0.957	0.953	0.954
PMMA	0.972	0.970	0.970	0.969	0.968	0.965	0.965	0.963	0.963
ABS	0.972	0.970	0.969	0.968	0.966	0.961	0.960	0.956	0.957

*MBF : MLC blocked field

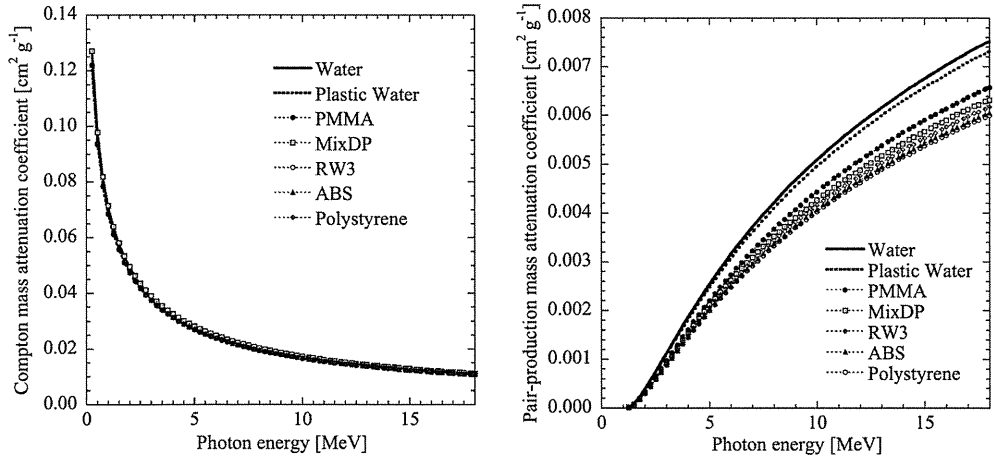

Fig. 1. (a) Compton mass attenuation coefficients and (b) pair-production mass attenuation coefficients for several solid phantoms.[16]

mined from the effective mass attenuation coefficient.

Depth and field size dependence

Figure 2 shows simulated photon energy spectra in water at various depths (a) on beam central axis for 10 MV photon beam with various size of open field (b) as an example of simulation results. Each spectrum was normalized to total photon fluence of the sampling region. E_{av} shows average photon energy determined from the photon spectrum.

As depth increase, photon energy was hardened by attenuation with a medium. The contribution of scattered photon was increased and E_{av} was decreased with increasing field size. Therefore, the beam hardening effect on the spectrum became small for large field.

Table 3 shows the depth scaling factors of the polystyrene for various depths and field sizes because it shows large

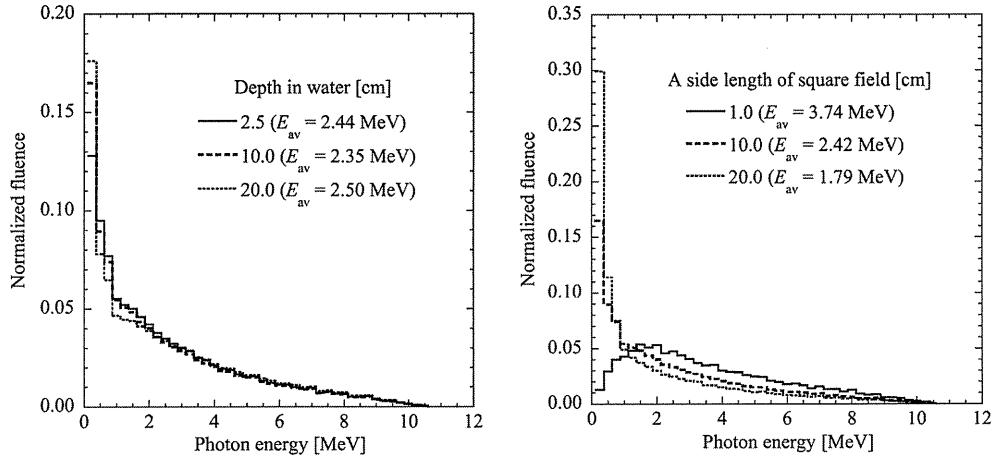

Fig. 2. Photon energy spectra in water for the 10 MV photon beam as a function of (a) depth and (b) field size at 10 cm depth. The each spectrum is normalized to total fluence of the sampling region. E_{av} shows average photon energies for each photon spectrum.

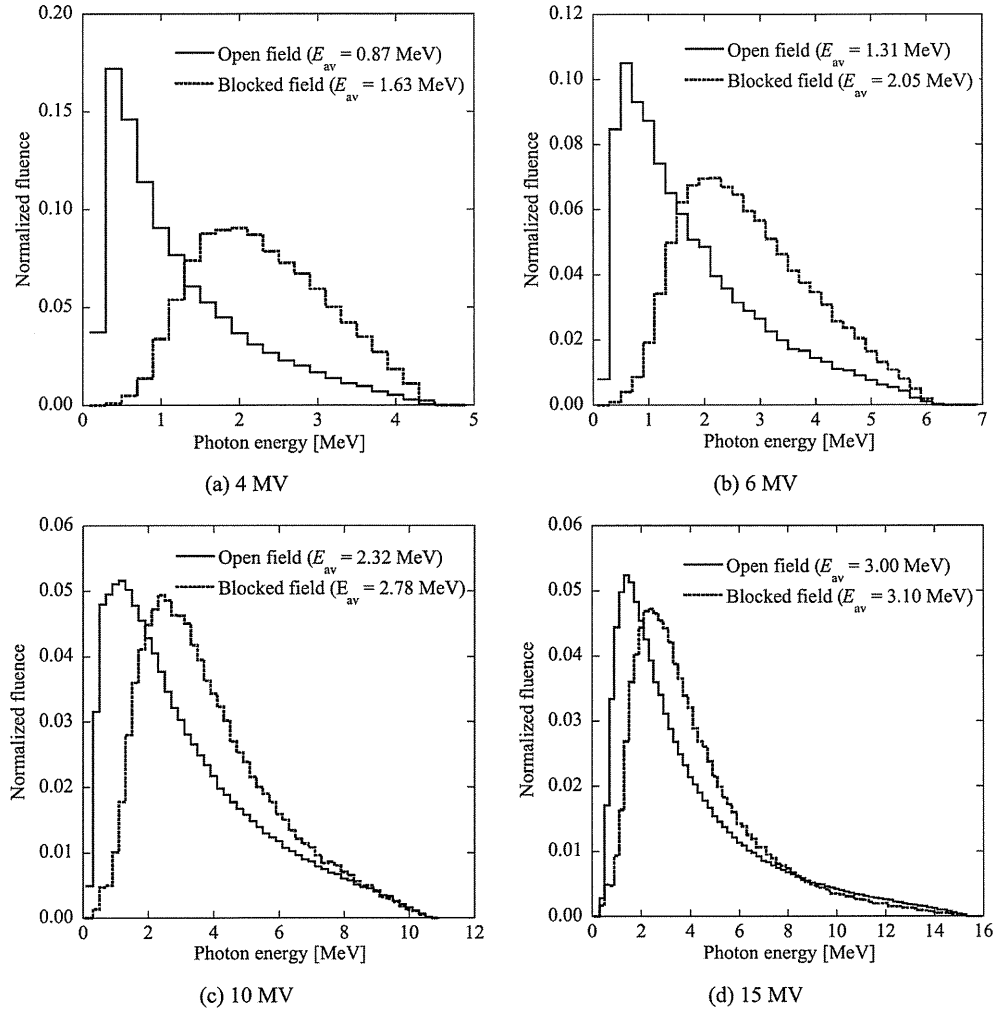

Fig. 3. Photon energy spectra in 2 cmϕ central area at phantom surface for the open field and blocked field for (a) 4 MV, (b) 6 MV, (c) 10 MV and (d) 15 MV. The each spectrum was normalized to total fluence of the sampling region.

Table 3. Depth scaling factors of the polystyrene for various depths and field sizes for 10 MV photon beam.

Depth [cm]	A side length of square field [cm]			
	1.0	5.0	10.0	20.0
2.5	0.956	0.957	0.958	0.958
5.0	0.956	0.957	0.958	0.958
10.0	0.955	0.957	0.958	0.958
15.0	0.955	0.956	0.957	0.958
20.0	0.954	0.955	0.957	0.958

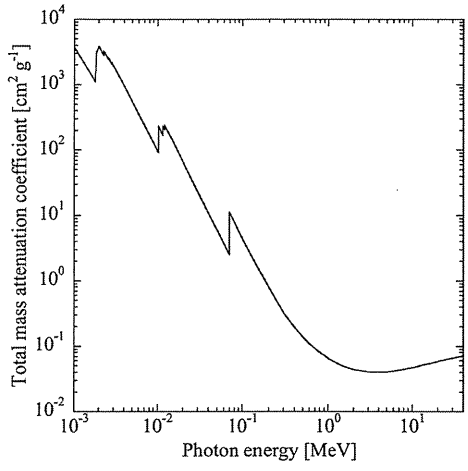

Fig. 4. The total mass attenuation coefficient for tungsten.[9)]

photon energy dependency. As mentioned above, the depth scaling factor is strongly depending on proportion of high energy part in the spectrum. The proportion of high energy part was constant even though depth and field size were changed, consequently, depth scaling factors were almost constant.

Influence of beam hardening effect by the MLC

Photon energy spectra at a phantom surface for open field and blocked field with the same jaw setting, 10 cm × 10 cm, are shown in Fig. 3. For all photon energies, the lower energy photons were removed by the MLC which tungsten has high mass attenuation coefficient for low energy photons as shown in Fig. 4. Furthermore, for 15 MV beam, reduction of high energy photons was also observed because tungsten has minimum mass attenuation coefficient at 4 MeV and the mass attenuation coefficient increases above 4 MeV.

The depth scaling factors for blocked field with 10 cm × 10 cm jaw setting are also tabulated in Table 2. For the Plastic Water, the depth scaling factor for the blocked field was equal to that of open field. On the other hand, the depth scaling factor of the RW3, MixDP, polystyrene, PMMA and ABS for the blocked field were obviously different from the relative electron densities. For the polystyrene, the difference of z_{pl} scaled by the relative electron density becomes 2.0 mm at 10 cm depth. This is because pair-production mass attenuation coefficients of these solid phantoms are different from water. However, the depth scaling factor for the blocked field was almost equal to the depth scaling factor for the open field. The z_{pl} determined from both scaling factors agreed within 0.2 mm at 10 cm depth.

Consequently, to minimize the error of the depth scaling for IMRT beams, the depth scaling factor should be obtained from the effective mass attenuation coefficient.

Conclusion

To clarify the accurate depth scaling method for IMRT beam, the variations of photon energy spectra for various radiation fields and depth scaling factors were determined. The results clarified that the depth scaling factor of Plastic Water were independent on photon energy. On the other hand, the depth scaling factors of the other phantoms were significantly different by photon energy. Therefore depth must be scaled by using presented depth scaling factor corresponding to photon beam energy.

The results also clarified that the ratio of effective mass attenuation coefficients of media to water are unaffected by whether open or blocked field. The presented depth scaling factor can also be used for IMRT beams.

In the future, this study can be used to clarify the effect of spectral variation for fluence scaling.

REFERENCES

1. Seuntjens J, *et al* (2005) Absorbed dose to water reference dosimetry using solid phantoms in the context of absorbed-dose protocols. Med Phys **32**: 2945–2953.
2. IAEA (2004) Absorbed Dose Determination in External Beam Radiotherapy: An International Code of Practice for Dosimetry Based on Standards of Absorbed Dose to Water. TRS 398. pp. 39–41. International Atomic Energy Agency, Vienna.
3. Pruitt JS and Loevinger R (1982) The photon-fluence scaling theorem for Compton-scattered radiation. Med Phys **9**: 176–179.
4. Onai Y and Kusumoto G (1959) Trial Production of a Water-Equivalent Solid Phantom Material. JJR **19**: 1012–1016. (in Japanese)
5. JSMP (2002) Standard Dosimetry of Absorbed Dose in External Beam Radiotherapy (Standard Dosimetry 01). pp. 165–172, Tsusho Sangyo Kenkyu Sha; Tokyo. (in Japanese)
6. Olivares M, *et al* (2001) Electron fluence correction factors for various materials in clinical electron beams. Med Phys **28**: 1727–1734.
7. Araki F, *et al* (2009) Monte Carlo calculations of correction factors for plastic phantoms in clinical photon and electron beam dosimetry. Med Phys **36**: 2992–3001.
8. Hine GJ (1952) The effective atomic numbers of materials for various gamma ray processes. Phys Rev **85**: 725.
9. Hubbell JH (1969) Photon Cross Sections, Attenuation Coef-

ficients and Energy Absorption Coefficients from 10 keV to 100 GeV. Natl Stand Ref Data Ser **29**.
10. Rogers DW, *et al* (1995) BEAM: a Monte Carlo code to simulation radiotherapy treatment units. Med Phys **22**: 503–524.
11. Heath E and Seuntjens J (2003) Development and validation of a BEAMnrc component module for accurate Monte Carlo modeling of the Varian dynamic Millennium multileaf collimator. Phys Med Biol **48**: 4045–4063.
12. AAPM (2001) Basic applications of multileaf collimators. AAPM Report No 72. pp. 9–10. Medical Physics Publishing, Wisconsin.
13. Sheikh-Bagheri D and Rogers DW (2002) Sensitivity of megavoltage photon beam Monte Carlo simulations to electron beam and other parameter. Med Phys **29**: 379–390.
14. Tzedakis A, *et al* (2004) Influence of initial electron beam parameters on Monte Carlo calculated absorbed dose distributions for radiotherapy photon beams. Med Phys **31**: 907–913.
15. Rogers DWO, *et al* (2000) NRC User Codes for EGSnrc. NRCC Report PIRS-702. pp. 64–68. National Research Council of Canada, Ottawa.
16. Berger MJ, *et al* (2005) XCOM: Photon Cross Section Database (version 1.3). [Online] Available: http://physics.nist.gov/xcom [2010, July 14]. National Institute of Standards and Technology, Gaithersburg, MD.

Received on May 13, 2010
Revision received on August 10, 2010
Accepted on September 2, 2010
J-STAGE Advance Publication Date: October 20, 2010